Geophysica (2004), 40(1-2), 3-13

On the Shape of the Fast Ice – Drift Ice Contact Zone

Robert V. Goldstein[1], *Nikolai N. Osipenko*[1] *and Matti Leppäranta*[2]

[1]Institute of Problems in Mechanics, Russian Academy of Sciences,
Prospect Vernadskogo 101-1, 119526 Moscow, Russia

[2]Division of Geophysics, University of Helsinki,
P.O Box 64 (Gustaf Hällströminkatu 2), FIN-00014 Helsinki, Finland

(Received: January 2003; Accepted: November 2004)

Abstract

The location and the geometry of the fast ice zone are examined in the Bay of Bothnia, Baltic Sea. Remote sensing images were collected from the fast ice – drift ice boundary zone showing that the fast ice boundary is formed of piecewise curved sections. A fracture mechanics model gives the ratio of wavelength to amplitude of these pieces as 3.6 while the observations suggest 4–6 for this ratio; the difference is likely due to the asymmetry between the strength of drift ice and fast ice. If the coastal morphology favours certain wavelengths, multiple smaller waves due to fracturing may develop onto the longer geometrically forced wave.

Key words: fast ice, boundary, fracture mechanics, Baltic Sea

1. Introduction

In a given basin the sea ice cover is divided into two dynamically different regions: the landfast ice zone, where the ice is by definition stationary apart from small viscoelastic strains, and the drift ice field where the ice moves under the influence of winds and currents at velocities up to 1 m/s. The boundary between them is dictated by the density of islands and grounded sea ice ridges and locates usually close to 10–20 m isobaths depending on the ice thickness and the bottom topography forms (e.g., *Zubov*, 1945; *Leppäranta*, 1981).

The location and geometry of the fast ice boundary is crucial in drift ice modelling since the characteristics of the ice motion are essentially different whether the motion is toward or away from the fast ice boundary. Also the fast ice boundary is the zone where heaviest ridging takes place and consequently largest ice forces occur. However, the physics of the fast ice formation has not been deeply studied, perhaps due to the severe complications caused by the topography of the costal zone. Very recently an extensive statistical study of the growth and decay of the fast ice zone in the Kara Sea has been made by *Divine* (2003). In earlier paper we analysed the kinematics and stress relaxation of drift ice in the coastal boundary zone (*Goldstein et al*., 2001). Here the formation of curved sections into the fast ice boundary is examined based on remote sensing images and fracture mechanics theory. To understand the fast ice zone and its evolution is crucial since it provides the boundary configuration for drift ice fields and because many human technological activities, such as drilling platforms and on-ice traffic roads, are concern this region.

2. Experimental data

A field experiment ZIP-97 (Zooming of Ice Physics, 1997) was performed in March 1997 in the Bay of Bothnia, northernmost basin of the Baltic Sea (*Haapala and Leppäranta*, 1997). The base was in the island of Hailuoto at the fast ice boundary, and the experimental work was focused on the dynamics of drift ice in the coastal boundary zone. Satellite and airborne remote sensing data as well as ground observations were collected for the ice kinematics and horizontal structure of the ice, including the geometry of the fast ice boundary.

Let us consider a large-scale SAR (Synthetic Aperture Radar) image of the ice cover in the Bay of Bothnia (Fig. 1). In this radar image fast ice appears as the dark (low backscatter) zone next to mainland on the right side (note that the black region on the upper left side is a lead with thin and smooth ice cover). The fast ice – drift ice boundary appears as a zone of ridged ice. We have several SAR images for February 20 – March 25 from the winter 1997, and in all the fast ice zone is about the same. But the stepwise evolution history is present in the high backscatter lines from this boundary toward coast, as also reported by *Dammert et al*. (1998) in an earlier study (1992) in the same basin.

The shape of this zone shows curved pieces with overall correspondence to the topography of the coast; also the bottom topography provides fixed tie points via grounded ridges (Fig. 2). However, separate detail parts of the boundary do not always match with the topographic macroprominences or hollows (Fig. 3). It is remarkable that the length to amplitude ratio of the curved pieces is nearly constant, 4 to 6.

We believe that the parameters of the piecewise curve characterise the largest scale of the fast ice – drift ice interaction. It is of deep interest to model the process leading to the formation of the regular shape of this interaction zone.

3. Theoretical model

For a theoretical approach, assume for simplicity that the curved pieces are sine form. Let us consider the formation of a specific sine curve contact boundary as a result of ridge formation in a region where this boundary is initially a straight line. At the scale of the wavelength of the sine curve, 50–100 km, the fracture zone can be modelled by a specific boundary condition at the contact line. Note that the contact line may only conditionally be separated since the ridge formation occurs within a strip of width larger than the size of ice floes. In particular, the width of a part of the contact zone given in *Haapala and Leppäranta* (1997: Fig. 42) is larger than the size of the largest ice floes. In this space scale atmospheric forcing is approximately constant and in the region of study the oceanic forcing is small. Therefore external forcing on the scale of the curvature of the fast ice boundary can be taken as constant.

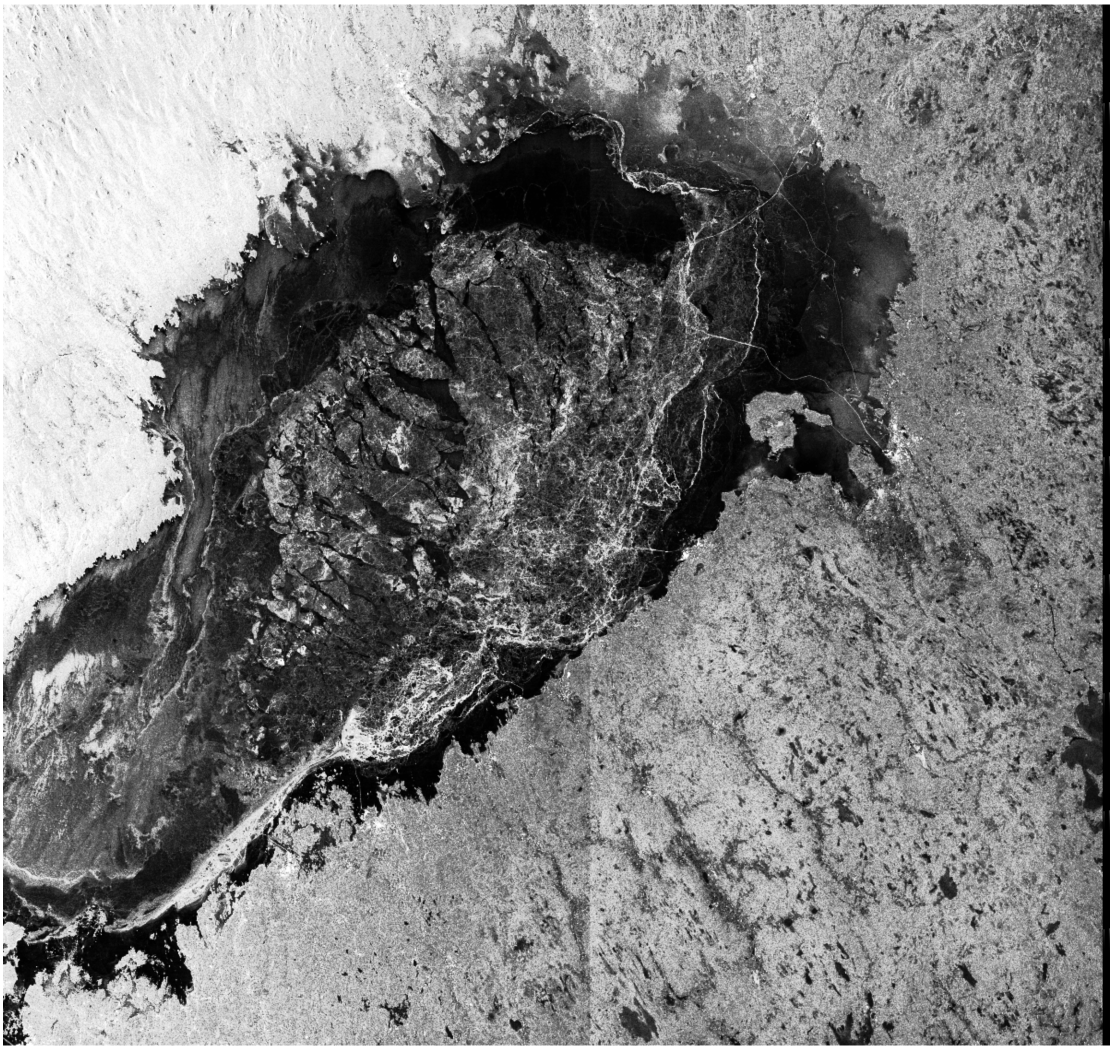

Fig. 1. The ice cover of the Bay of Bothnia on 17 March 1997 during the ZIP-97 experiment, in a section of Radarsat SAR image (Sandven et al., 1999). © Canadian Space Agency.

If we consider the region of the contact interaction as a whole, its scale is essentially larger as compared to the scale of the local contact zone where single ridges are formed. The plane orientation of the contact region is important in this larger scale. The conditions of ridging depend on the presence of the shear component in mutual displacement of the interacting ice masses. Note, that speaking about the ridging conditions we consider the energy capacity of the deformation and fracture processes at the scale of the whole contact line instead of the conditions of formation of a separate local ridge. Hence, a model of ice cover fracture at the scale of multiple ridge formation (i.e. at the scale of the whole contact line) generally differs from a model of single ridge formation.

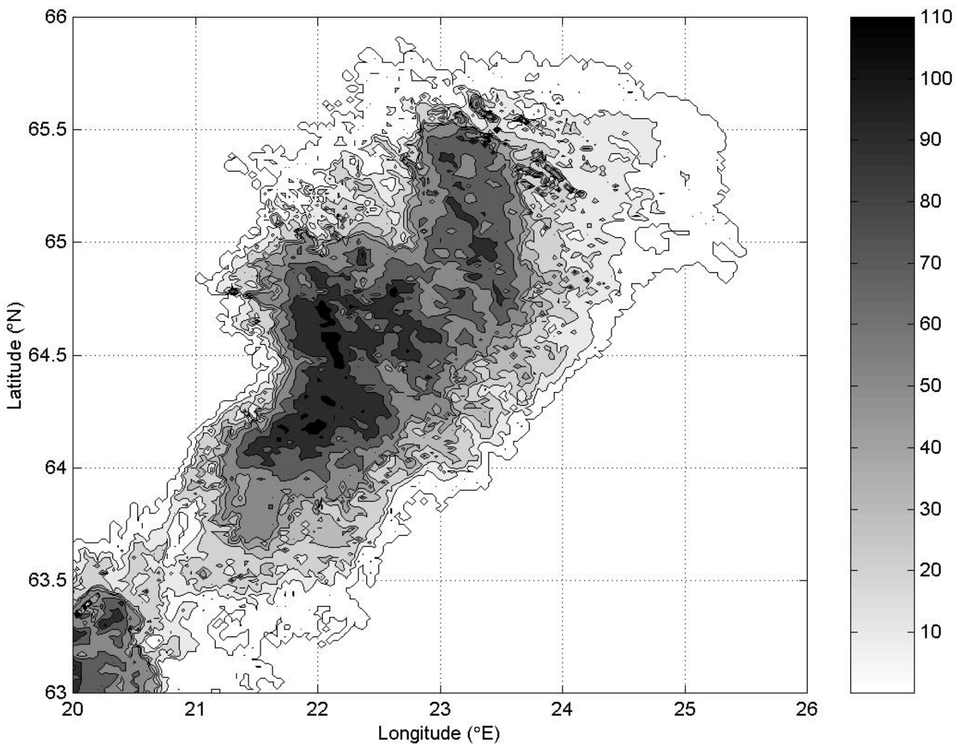

Fig. 2. Bathymetric chart of the Bay of Bothnia.

Later on we consider an example of such model, which is related to the variant of multiple fracture at the contact line when the fracture conditions depend on the macro orientation of the contact line.

A qualitative model of the contact zone formation is the following. Prior to the contact the ice cover is a set of weakly connected large ice floes. As a result of the interaction, different forms of elongated ridges form. The conditions of the limit state for different orientation of the ice cover plane along the contact line are different. For instance, it is known that ridge formation needs lower normal tractions in the contact zone if relative sliding of the edges of ice floes occurs. Hence, the fracture conditions (the value of the specific load) at the contact line for the ridged ice depend on the local orientation of this line relative to the direction of the main compression (here the term “local” means local at the macroscale, i.e. on a part of the contact line much larger than its thickness).

As mentioned above, shear stresses acting along the contact line make ridge formation easier. One may assume that the curvilinear shape of the contact line is chosen such way that ridge formation will occur along this line in local shear. Then the initial rectilinear contact line becomes curvilinear with a spatially periodic variation of its curvature. The final shape of the contact line is adjusted by the specific form of the dependence of the limit tractions at the contact line on the orientation and duration of the process.

Let us consider the fast ice – drift ice interaction process using some simplifying assumptions. The mechanical properties of the fast ice and drift ice will be assumed the same (the case of symmetric fracture and, hence, symmetric possible contact line). In particular, assume that the contact line becomes sine-shaped at its deviation from the initial straight line (Fig. 3).

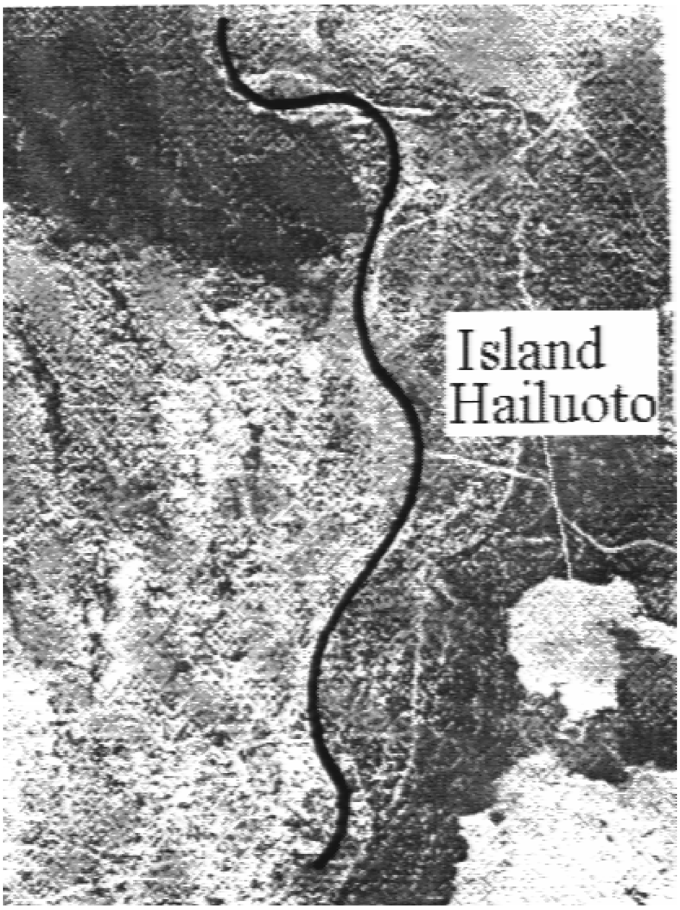

Fig. 3. A close-up of the fast ice boundary region at Hailuoto island, from Fig. 1.

$$y = A \cos kx \tag{1}$$

where x and y are the co-ordinates of the sine curve, and k and A are its wavenumber and amplitude, respectively. Assume then that A is related to the displacement of drift ice along the contact line when intensive ridging occurs

$$A \sim \Delta \sim vt \tag{2}$$

where v is the drift ice speed along the contact line and t is the time. For typical conditions in the basin, we have $v \sim 0.1$ m/s, $t \sim 1$ day, and thus $A \sim 10$ km (e.g., *Leppäranta*, 1981; *Leppäranta et al.*, 2001).

Considering the fracture process at the scale of the whole contact line we assume that the fracture condition at the normal contact (i.e. the vector of mutual displacements of ice massifs in contact is oriented transverse to the contact line) has the following simple form: $\sigma \approx \sigma_0 =$ constant. The fracture condition becomes dependent on the angle of orientation if the contact region has another orientation. Let us write the interrelation between the limit stress and orientation angle as follows

$$\sigma(\alpha) \approx \sigma_0 f(\alpha) \tag{3}$$

where α is the plane angle between the normal to the contact line and the vector of mutual displacement. The form of the function f may vary in depending on the range of the angle α. For instance, the contact line given in Fig. 3 is characterized by smallness of the angle α.

For small angles α we assume that the condition of macrofracture (which is related to the variation of the resistance to mutual displacement of the ice massifs in contact) is determined by the variation of normal load on the contact zone, $\Delta\sigma$, as compared to the level under normal contact. One may estimate $\Delta\sigma$ as the difference between the stress σ_0 and projection of the normal component of the stress σ_n (see Fig. 4a). Then we obtain $\Delta\sigma \sim k\sigma_0 \sin^2\alpha$ for small α, where k is a coefficient of order 1.

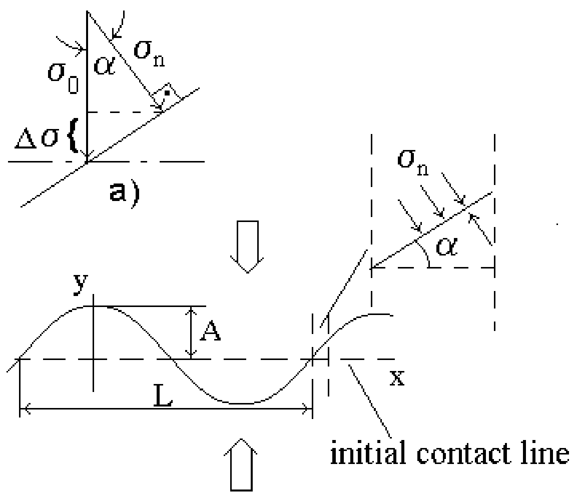

Fig. 4. The shape of the contact line.

The condition of fracture (Eq. 3) can be written as

$$\sigma \approx \sigma_0 (1 - k \sin^2\alpha) \tag{4}$$

In case of $k \approx 1$, we have $\sigma \approx \sigma_0 \cos^2\alpha$. It can be obtained, e.g., within the framework of the following schematic model of macrofracture at the scale of the contact zone.

Stress relaxation occurs in the contact zone by reconstruction of the initially homogeneous fast ice, mainly associated with ridging. Let us evaluate the ridging conditions at the scale of the contact zone. In this case the motions of separate ice floes may include rotation to find a favourable contact. Assume that the ridging condition is mainly determined by the possibility for a separate ice floe to go out from the plane of the ice cover. This mechanism is appropriate to multiple ridge formation in the fast ice.

Let us perform some simple transformations. For small values of the angle α, Eq. (3) can be simplified to

$$\sigma \sim \sigma_o(1-\sin^2\alpha) \sim \sigma_o(1-tg^2\alpha) \sim \sigma_o\left(1-\left(\frac{\mathrm{d}y}{\mathrm{d}x}\right)^2\right) \tag{5}$$

and, according to Eq. (1), $\mathrm{d}y/\mathrm{d}x = -Ak\sin kx$. Assume that the parameters of the sinusoidal contact line are determined by the minimum condition for the work of fracture. This work at the ¼ wavelength equals

$$Q = \int_o^{\pi/2k} \sigma \cdot y(x) \cdot \mathrm{d}x \tag{6}$$

where the ice thickness is assumed to be equal to 1. Then from Eqs. (1) and (5) we obtain

$$Q \sim A\sigma_o \int_o^{\pi/2k} (1-A^2k^2\sin^2 kx)\cos kx dx$$

$$Q \sim A\sigma_o\left(\frac{1}{k}+\frac{A^2k}{3}\right) \tag{7}$$

By incorporating the minimum condition of the work of fracture, we have

$$\frac{\partial Q}{\partial k}=0\ ;\quad \frac{\partial Q}{\partial k} = A\sigma_o\left(-\frac{1}{k^2}+\frac{A^2}{3}\right)=0\,,\ \ k=\frac{\sqrt{3}}{A} \tag{8}$$

Then the relation for the sinusoid wavelength can be written as follows

$$L=\frac{2\pi}{k}=\frac{2\pi}{\sqrt{3}}\cdot A \sim 3.6A \tag{9}$$

Eq. (9) shows that the sine wave length is only related to its amplitude in this model. This relation being also linear, the ratio of the contact line wavelength to its amplitude is a constant of 3.6. Taking into account Eq. (2) we obtain $L \sim 3.6vt$.

It is difficult to have a continuous variation in the wavelength of an active contact line with an increase of the ice motion amplitude. A more realistic scenario is to fix the initial wavelength by e.g. boundary conditions. Let us consider the variation of the specific work in the region of the active contact as the amplitude of the ice motion increases at a fixed wavelength. Eq. (7) can be rewritten using the parameter $A^* = A/L$ equal to the ratio of the amplitude of the ice motion to the wavelength of the contact contour:

$$Q = A^* \sigma_0 L^2 \left(\frac{1}{2\pi} + \frac{2\pi}{3} (A^*)^2 \right) \tag{10}$$

The function $Q(A^*)$ is linear at small A^* (in the initial period of time), see Fig. 5.

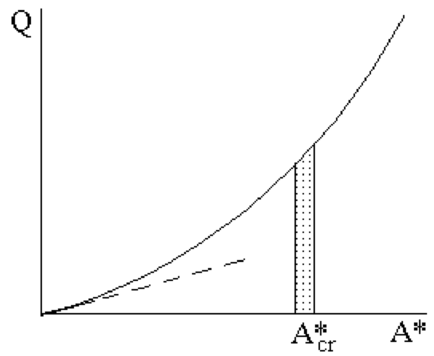

Fig. 5. Scheme of the dependence between the work of ice cover fracture and amplitude A^*.

Hence, two characteristic regimes of energy expenditure exist for the present model. A high level is needed for large ice displacements when further growth of the contact zone with the initial contour wavelength becomes disadvantageous. One may assume that just this effect leads to a replacement of one contact zone by another for which the loading cycle is repeated. This replacement can be accompanied by a contact line contour (such that the wavelength will increase) in dependence on the boundary conditions. If the wave number response remains unchanged, then one can observe an embedded contour in another sinusoidal contour, which occur sequentially with the ice motion. Critical conditions of the contact zone replacement can be determined by comparing the energy expenditure related to the appropriate mechanisms of fracture initiation and growth of the preceding contact zone.

Let us estimate these conditions using the assumption that the change of the regimes of the energy expenditure with the ice motion growth leads to the fast attaining of the critical state, i.e. the critical level A^* is placed near the range where the both mechanisms provide approximately equal energy contribution (this range is marked in Fig. 5 by the value A^*_{cr}). Within the framework of this assumption we obtain from Eq. (10)

$$\frac{1}{2\pi} \approx \frac{2\pi}{3} \left(A^*_{cr} \right)^2 \tag{11}$$

Hence $A^*_{cr} \approx \sqrt{3}/2\pi$. This result coincides with Eq. (8), i.e. attaining the optimality conditions according to Eq. (9) is associated with the start of the sharp increasing of the resistance to the further ice motion.

Returning to the example given in Fig. 1, note that the clamping of separate points of the curved contact line can be associated with a quasiperiodic location of the island groups in the northern part of the Bay of Bothnia. One can see several contours of the contact zones. It is possible, according to the present model, that these contours may be formed sequentially as a result of the contour replacement. Hence, the observed amplitudes of the waves need to be close to the critical one.

The estimates confirm that the regime of fracture along the fast ice – drift ice boundary is characterised by the formation of a curvilinear contact line with the constant proportions of its geometric parameters at the macroscale. The ratio of wavelength to amplitude is 4–6 according to the observations while the estimate of 3.6 is obtained from the present theory based on sinusoidal symmetry. Note, that the value 3.6 is the lower limit estimate of this ratio. If the mutual displacements of the ice cover parts being in contact are not large (the amplitude is small), then the ratio *L/A* will be larger as it was observed in field conditions. Notice, that the conditions of local fracture for the fast ice and drift ice can be different. If the fracture resistance of the interacting ice edges is different, then the more weak edge will mainly be fractured. Hence, the scheme of fracture and the contact line shape lose their symmetry. The above approach can be modified to model that case. An appropriate modification will be considered separately.

Qualitatively one may assume that in that case the amplitude of the fracture front deviation from the initial straight line will decrease. To illustrate this assumption let us consider an asymptotic case of a large difference of the strength of the interacting drift ice and fast ice. Then the ice of high strength will not be fractured at all and as a result the shape of the contact line will remain unchanged. Indeed, if the fracture energy of the drift ice under the normal contact is independent on the local orientation of the contact area element (this is inherent for the level ice), then the fracture condition can be written as follows

$$\sigma \sim \sigma_o (\cos^2 \alpha + b) \tag{12}$$

where b is the weight coefficient for the drift ice fracture at the contact with the fast ice. Then performing transformations similar to what was made above, we obtain instead of Eq. (8) the following relation for the wavelength – amplitude relationship

$$L \sim A \frac{2\pi\sqrt{1+b}}{3} \tag{13}$$

Again the ratio *L/A* is constant but now its value depends on the realised combination of fracture mechanisms at the contact line. This would in fact explain why the observed *L/A* ratio was larger than the prediction by the symmetric theory.

The transition from one wavelength of the contact line to another one, when the fast ice push *vt* increases, should occur in a jump-like manner. Indeed, initially optimal wavelength becomes more and more non-optimal with increasing of the fast ice push. Hence, one may expect that the traces of these intermediate stages of the final contact line formation partly remain in the contact zone. In particular, such traces can be identified in Fig. 1. These traces enable to reconstruct the history of the fast ice – drift ice interaction.

4. Conclusions

The location and the geometry of the fast ice zone have been examined in the Bay of Bothnia, Baltic Sea. Remote sensing images were collected from the fast ice – drift ice boundary zone in the experiment ZIP-97 in winter 1997. These images showed the fast ice boundary forming of piecewise curved sections. A model was presented for this boundary curve assuming the geometry of a half sine wave for each curved piece, and the shape was then solved based on minimising the work on fracturing. According to the model the ratio of wavelength to amplitude of these pieces is constant and equal to 3.6. If the strengths of fast ice and drift ice are different, the sine symmetry of the curve is broken and the amplitude becomes smaller. If the coastal morphology favours certain wavelengths due to e.g. distance between islands or shoals, multiple smaller waves may develop onto a morphologically guided larger wave.

The results of this work in all shows promises for approaching the fast ice boundary problem from fracture mechanics. Only the Bay of Bothnia has been examined but the methodology as such is applicable to other seas.

Acknowledgement

Matti Leppäranta has been supported by the Academy of Finland for a sabbatical leave 2002–2003.

References

Dammert, P.G., M. Leppäranta and J. Askne, 1998. SAR interferometry over Baltic sea ice. *International Journal of Remote Sensing*, **19**(16): 3017–3037.

Divine, D., 2003. *Peculiarities of Shore-Fast Ice formation and Destruction in the Kara Sea.* PhD thesis, Geophysical Institute, University of Bergen, Norway.

Goldstein, R., M. Leppäranta and N. Osipenko, 2001. On the formation of large scale structural features. In J.P. Dempsey and H.H. Shen (eds.), *IUTAM Symposium on Scaling Laws in Ice Mechanics*, pp. 324–334. Kluwer Academic Publishers, Dordrecht, the Netherlands.

Haapala, J. and M. Leppäranta (eds.), 1997. ZIP-97 Data Report. Report Series in Geophysics, No. 37, 123 p. University of Helsinki Department of Geophysics. Helsinki.

Leppäranta, M., 1981.On the structure and mechanics of drift ice in the Bay of Bothnia. *Finnish Marine Research* **248**, 3–86.

Leppäranta, M., Z. Zhang, J. Haapala and T. Stipa, 2001. Sea ice mechanics in a coastal zone of the Baltic Sea. *Annals of Glaciology* **33**, 151–156.

Sandven, S., M. Lundhaug, Ø. Dalen, K. Kloster and V. Alexandrov, 1999. Satellite observations. In: *Local Ice Cover Deformation and Mesoscale Ice Dynamics. Part 1: Final Scientific Report* (ed. K. Riska and J. Tuhkuri), p. 317–331. Rep. M-242, Ship Laboratory, Helsinki University of Technology, Espoo, Finland.

Zubov, N.N., 1945. *L'dy Arktiki* [Arctic Ice]. Izdatel'stvo Glavsermorputi, Moscow.